Metal-semiconductor transition like behavior of naphthalene-doped single wall carbon nanotube bundles

Fitri Khoerunnisa[a], Aaron Morelos-Gomez[b], Hideki Tanaka[c], Toshihiko Fujimori[d], Daiki Minami[d], Radovan Kukobat[d,e] ,Takuya Hayashi[e] , S.Y. Hong[f], Y.C. Choi[f], Minoru Miyahara[c], Mauricio Terrones[g], Morinobu Endo[b] and Katsumi Kaneko*[d]

Naphthalene (N) or naphthalene-derivative (ND) adsorption-treatment varies evidently the electrical conductivity of single wall carbon nanotube (SWCNT) bundles over the wide temperature range due to charge transfer interaction. The adsorption treatment of SWCNT with dinitronaphthalene molecules enhances the electrical conductivity of the SWCNT bundles by 50 times. The temperature dependence of electrical conductivity of N- or ND-adsorbed SWCNT bundles having the superlattice structure suggests metal-semiconductor transition like behavior near 260 K. The ND-adsorbed SWCNT gives a maximum in the logarithm of electrical conductivity vs. T^{-1} plot, which may occur after the transition to a metallic state and be associated with a partial unraveling of the SWCNT bundle due to an evoked librational motion of the moieties of ND with elevation of the temperature.

1 Introduction

Single wall carbon nanotube (SWCNT) has a wide range of the electronic property from semiconductor to metal depending on the chiral indexes which describes the rolling up structure of graphene. As all carbon atoms of SWCNT are exposed to the surface, the geometrical surface area is 2630 $m^2g^{-1}$and SWCNT is intrinsically surface sensitive.[1] Even exposure of an inert gas gives an influence on the electrical conductivity of SWCNT with the atom collision-induced distortion in the graphene wall,[2] although adsorption of electron donor or electron acceptor gases markedly changes the electrical conductivity of SWCNT.[3-5] SWCNTs form an ordered bundle structure of a 2D hexagonal superlattice due to the inter-tube dispersion interaction.[6,7] Therefore, if we remove caps from SWCNT by oxidation-treatment, the open SWCNT bundles have three kinds of adsorption sites for molecules and atoms of the internal tube spaces, interstitial pore spaces and groove sites.[8] Here the internal tube space is in each open SWCNT, the interstitial pore spaces between three SWCNTs and the groove sites are at the area where two SWCNTs are arrayed on the external surface of the bundle. The internal tube spaces of open SWCNT bundle is available for adsorption of various molecules whose size is smaller than the effective size of the tube spaces. The in-pore superhigh pressure effect of internal tube spaces of SWCNT is clearly evidenced recently. Solid KI transforms into high pressure phase at 1.9 GPa in the bulk conditions; the high pressure phase transformation is induced by introduction of KI nanocrystals in the carbon nanotube spaces even below 0.1 MPa.[9] It is known that solid sulfur having eight member-ring structure, being a typical insulator, converts to 2D network structure consisting of 1D sulfur chains above 90 GPa. Introduction of sulfur atoms in the internal nanospaces of SWCNT below 0.1 MPa gives atomically 1D sulfur chain crystal of metallic nature, indicating the intensive compression effect for sulfur

[a]*Department of Chemistry, Indonesia University of Education, Bandung 40154, Indonesia*
[b]*Aqua Eco Center, Shinshu University, Nagano 380-8553, Japan*
[c]*Department of Chemical Engineering, Kyoto University, Nishikyo, Kyoto 615-8510, Japan*
[d]*Center for Energy and Environmental Science, Nagano 380-8553, Japan*
[e]*Department of Electrical Engineering, Shinshu University, Nagano 380-8553, Japan*
[f]*Research and Development Center, Hanwha Nanotech, Incheon 403-030, Republic of Korea*
[g]*Department of Physics, Pennsylvania State University, University Park, Pennsylvania 16802,USA*

atoms corresponding to 90 GPa at least.[10] As the interstitial nanopores offer the smallest pores and has the deepest interaction potential wells, accessible molecules can be strongly adsorbed there.[11] If SWCNT is capped and close, the internal spaces are not available for molecules and atoms and thereby only the interstitial pores can accept atoms and molecules. When the interaction between the interstitial pore and atoms or molecules is strong enough to vary the SWCNT bundle structure, the intercalation-like structure similar to intercalation graphite[12] is formed. Br_2, K, TCNQ, and pentacene etc are doped in the SWCNT bundles by vaporization of these intercalants in the gas phase at high temperature, giving the intercalation structures.[13,14] Intercalation structure formation changes remarkably the electrical conductivity of the SWCNT bundles. The well crystalline SWCNTs give sharp X-ray diffraction patterns of the super lattice of the bundle,[6,7] although each SWCNT may perform a librational motion in the bundles and a weak inter-tube coupling causing a slight change in the electronic structure around the Fermi level according to the theoretical studies.[15] Thus, the intercalation-type modification of the SWCNT bundles is effective for tuning the electronic properties as well as intercalation of graphite.

On the other hand, adsorption of C_{60} and polycyclic aromatic hydrocarbon (PAH) molecules on SWCNT bundles in the liquid phase induces their intercalation-like structure, where the charge transfer interaction occurs between PAH molecules and SWCNT.[16,17] In our preceding study, naphthalene-adsorbed SWCNT has the intercalation structure according to the X-ray diffraction and the ultraviolet photoelectron spectroscopy shows an explicit increase of the density of state at the Fermi level which indicates pseudo-metallic state.[18] In this study we modify SWCNT bundles with naphthalene and its derivatives of different electronic property using liquid phase adsorption. The temperature dependence of dc electrical conductivity of the naphthalene derivative (ND)-adsorbed SWCNT was measured, suggesting the molecular motion-mediated unique temperature dependence of the electrical conductivity in addition to the Mott transition like behavior which has been observed in transition metal oxides and disordered solids.

2 Experimental and computation procedures

SWCNT produced from graphite with arc-discharge method by Hanwha Nanotech Co. was used in this study. The SWCNT was purified with 1 M HCl for 20 h at room temperature to remove metallic impurities and dried at 373 K after washing. Then the SWCNT samples were annealed at 1473 K in Ar for 30 min to remove amorphous carbons. The content of metal oxide impurities was 3 wt. % by thermal gravimetric analysis in a flow of O_2-N_2 mixed gas; the graphite remains according to X-ray diffraction measurement. The diameter of the SWCNT is 1.3 to 1.5 nm and the bundle size is 20 nm to 30 nm in average according to the preceding study.[19] Liquid phase adsorption of naphthalene (N) and its derivatives (ND) in the SWCNT bundle was carried out using the toluene solution at 298 K. Here, 1,5-dinitronaphthalene (DNN, $C_{10}H_6N_2O_4$) and 1,5-dihydroxynaphtalene (DHN, $C_{10}H_8O_2$) were used as the ND agent. Here DNN and DHN should work as an electron acceptor and an electron donor, respectively.[20] The dispersed SWCNT samples were filtrated and rinsed by toluene to remove any non-adsorbed N and ND molecules. The ND-adsorbed SWCNT samples were dried before characterization under vacuum at 323 K and 10 mPa for 24 h. The ND adsorption amount was determined from the concentration change of ND molecules in the solution using a UV-Vis-NIR spectrometer (JASCO; V-670). Raman spectra were obtained with 532 nm and 785 nm excitations, using a single-monochromator micro-Raman spectrometer in back scattering configuration (inVia Raman Microscope, Renishaw). The surface coverage of SWCNT with N or ND molecules was controlled to be 0.30 ± 0.10, which was determined by the surface area of SWCNT from N_2 adsorption at 77 K and the area occupied by N or ND molecules using their molecular area. The optical absorption spectra of the SWCNT samples were collected using the UV-Vis-NIR spectrometer. The dc electrical resistance measurements of the SWCNT Bucky paper form were performed by the four probe method using a physical properties measurement system (model 600: Quantum Design) over the temperature range of 2 K to 340 K. The melting temperatures of DNN and DHN were measured using a DSC system with 10 $Kmin^{-1}$ after calibration with In (DSC 8500: Perkin Elmer). The plausible configuration of DNN molecules in an interstice of the SWCNT array

was simulated with GCMC simulation using the structural parameters of the bundle estimated from X-ray diffraction experiment; in the simulation (12,10) SWCNT of tube diameter of 1.495 nm was used. The simulation details are given in supporting information. We computed the electronic energy levels of naphthalene and ND molecules and the density of states of the (17,0) SWCNT of tube diameter of 1.350 nm with ab initio density functional theory as implemented in the SIESTA code. The computational method is described in supporting information. Here, both SWCNTs are semiconductive.

3 Results and Discussion

The purified SWCNT is almost closed even after the above-mentioned purification from N_2 adsorption measurement at 77 K; the surface area of SWCNT is 330 m^2g^{-1}, indicating that SWCNT is closed.[19] All SWCNT samples are mixture of metallic and semiconducting SWCNTs due to the feature of the G^- Raman band.[19] Fig. 1 shows SEM images of SWCNT before the adsorption treatment and DHN-adsorbed SWCNT bundle. We can see very bold SWCNT bundles and these SWCNT bundles are randomly entangled with each other before adsorption treatment. The SEM image of DHN-SWCNT is completely different from that of SWCNT before the treatment; the bundle size decreased markedly by the adsorption treatment, indicating insertion of DHN molecules in the intertube spaces. Similar images were obtained for N- and DNN-SWCNTs. Fig. 2 shows the X-ray diffraction patterns of SWCNT, N-SWCNT, DNN-SWCNT and DHN-SWCNT. The diffraction pattern of SWCNT has sharp peaks coming from the well-ordered bundle structure of the hexagonal symmetry; the predominant peak at 2.72° is assigned to the 10 peak, the other peaks at 4.40°, 7.06° and 9.56° correspond to the reflections from 11, 20 and 21 superlattice planes of the bundles, respectively. The inset shows the magnified X-ray diffraction patterns of the 10 peak for all samples. The sharp peak at 11.90° is caused by the reflection from the 002 plane of graphite as the impurity. The diffraction patterns consisting of sharp peaks of the SWCNT dramatically change after the adsorption treatment with N and ND molecules. The intensity of all peaks coming from the ordered bundle structure decreases markedly, accompanying an explicit broadening. In particular, the 10 peak shows the greatest change, giving a lower diffraction angle shift corresponding to the expansion of the interlayer spacing by 0.12 nm for DNN-SWCNT, 0.063 nm for DHN-SWCNT and 0.10 nm for N-SWCNT. The magnified 10 peaks in the inset show evidently this change. Accordingly, the ordered SWCNT bundle structure should be partially broken to embrace N or ND molecules, coinciding with SEM observation. Fig. 3 shows optical absorption spectra of the adsorption treated and non-treated SWCNT samples. This SWCNT sample is a mixture of metallic and semiconductive SWCNTs and we can observe the interband transitions due to metallic and semiconductive band structures. The spectrum of SWCNT has three broad bands due to the M_{11}, S_{11} and S_{22} transition. Here, M_{11} is the transition between the first van Hove singularities of metallic SWCNT, whereas S_{11} and S_{22} are the transitions between the first and second van Hove singularities of semiconductive SWCNT, respectively.[21,22] The adsorption treatment induces an intensive hyperchromic effect for M_{11}, S_{22} and S_{11} bands and an explicit red shift of three bands by 7-13 nm for M_{11}, 13-18 nm for S_{22}, 16-41 nm for S_{11}. The intensive hyperchromic effect and explicit red shift of three bands clearly evidence the mixing of wave functions of N or ND molecules and SWCNT regardless of metallic or semiconductive SWCNT; there should be a marked charge transfer interaction between naphthalene or ND and SWCNT. The naphthalene or ND adsorption treatment, however, did not give a marked change in the radial breathing mode (RBM) and G^-band frequencies[23]: G^+-band (cm^{-1}) by 532 nm excitation, SWCNT: 1592, N-SWCNT: 1594, DHN-SWCNT: 1594 and DNN-SWCNT: 1592, RBM (cm^{-1}) by 532 nm excitation, SWCNT: 168, N-SWCNT: 174, DHN-SWCNT: 174 and DNN-SWCNT: 170 (Fig.2S(A)). The higher frequency shift of DNN-SWCNT is slightly different from that of N- and DHN-SWCNT. We obtained similar results by excitation with 785 nm, as shown in Fig.2S(B). The Raman spectroscopic data are not clearly understood yet. Figure 4 shows the temperature dependence of electrical conductivity of the SWCNT samples. The absolute electrical conductivity of the SWCNT sample is different from each other. The DNN-adsorption increases remarkably the electrical conductivity and the electrical conductivity is larger than that of SWCNT by 50 times. N-adsorption increases the electrical

conductivity slightly, whereas DHN-adsorption gives just a little decrease of the electrical conductivity. The extrapolation of the approximated linear plot above 125 K to the vertical axis gives the following electrical conductivity (See Fig. 5): SWCNT; 3.2 x 10^3 Sm^{-1}, N-SWCNT; 5.1 x 10^3 Sm^{-1}, DNN-SWCNT; 1.7 x 10^5 Sm^{-1} and DHN-SWCNT; 2.8 x 10^3 Sm^{-1}. Thus, the DNN-adsorption treatment is quite efficient to enhance the electrical conductivity of SWCNT bundles. The logarithm of electrical conductivity vs. T^{-1} plot is almost linear in the lower temperature region and deviates upward near an ambient temperature. The electrical conductivity change should be correlated with the electronic property of N, DNN and DHN molecules. It is assumed that a DNN molecule of an electron acceptor pulls an electron from SWCNT to create a hole, being a charge carrier, to enhance the electrical conductivity, while a DHN molecule of an electron donor donates an electron to SWCNT to annihilate a hole in the SWCNT. Thus, the concept of the electron donor and acceptor can explain qualitatively the electrical conductivity change through the adsorption treatment of the SWCNT bundles. However, the above explanation must be supported by the computational study on the electronic structure of the ND-adsorbed SWCNT. The preliminary computational results of the density of state of the semiconductive (17,0) SWCNT and the energy diagrams of three molecules are shown in Fig.1S. The HOMO level of DHN is slightly higher than the Fermi level, whereas the HOMO levels of naphthalene and DNN are lower than the Fermi level. On the other hand, the LUMOs of DNN and naphthalene are higher than the Fermi level by about 1 eV and 3 eV, respectively. In case of charge transfer complexes between donor and acceptor molecules, the LUMO-HOMO energy difference of 1-3 eV between acceptor and donor molecules induces a predominant charge transfer interaction at the presence of the sufficient orbital overlapping according to the molecular orbital study.[24] If we apply the charge transfer interaction in the molecules to the molecule-SWCNT interaction, DNN whose LUMO is closer to the Fermi level of SWCNT should induce a stronger charge transfer interaction than naphthalene. Consequently we conjecture that the adsorbed DNN molecules pull the electrons from SWCNT to create the holes more efficiently than naphthalene molecules, although the systematic study on the electronic interactions between ND or naphthalene and SWCNT with the DFT computational method is necessary in future. The above distinct electrical conductivity change of the SWCNT bundles with adsorption of naphthalene or ND molecules suggest the formation of the partial intercalation structure between SWCNT bundle and N or ND molecules. The interesting behavior is observed in the electrical conductivity near ambient temperature, as shown in Fig.5. The electrical conductivity σ of N-SWCNT becomes almost constant above 250 K, being similar to a metallic conductor, whereas the $\log \sigma$ vs. T^{-1} plots of DNN-SWCNT and DHN-SWCNT have a gentle maximum around 250 K and 270 K, respectively. Even the $\log \sigma$ vs. T^{-1} plot of SWCNT is slightly upward-deviated around 250 K. The $\log \sigma$ vs. T^{-1} plot of N-SWCNT agrees with the pseudo-metallization shown by the preceding UV photoelectron spectroscopic study.[18] As the $\log \sigma$ vs. T^{-1} relation below the bending temperature is almost linear, the SWCNT samples are assumed to be semiconductors below the bending temperature. Consequently, phenomenologically the observed behavior in N-SWCNT suggests a metal-semiconductor transition which has been observed in transition metal oxides, covalent semiconductors containing impurities and disordered solids, which have localized electrons.[25,26] We infer that the unusual $\log \sigma$ vs. T^{-1} relations of DNN- and DHN-SWCNT are also associated with the semiconductor-metal transition as well as N-SWCNT. Here we must remind that the electrical conductivity was measured using the SWCNT Bucky paper.

The SWCNT Bucky paper consists of many bundles and thereby there are two kinds of barrier for carrier transport. One is the SWCNT-SWCNT contact and another is the bundle-bundle contact. The electric charges must carry mainly through the metallic SWCNTs in the bundle and the charge carriers in the bundle should behave as localized ones and then such localized carriers must transport the neighbor bundle through the contact. The Mott variable range hopping mechanism for transition metal oxides and disordered solids can be applicable to explain the electrical conduction behavior of the SWCNT bundle.[10,27-29] Snoussi et al showed that the localization length is 4-11 nm being the boundary size of the bundle for the SWCNT thin film using the Mott theory.[27] Fig. 6 shows the 3D variable range hopping plots of the temperature dependence of electrical conductivity of all SWCNT samples over the wide temperature range from 2 K to 340 K. The 3D variable range hopping plots

are almost linear over the wide temperature range except for the higher temperature range. Here, the 3D variable range hopping plots give the best fit compared with the plots of other dimensions. Therefore, the electron conduction network should be three-dimensional, agreeing with the 3 D entangled structure of the SWCNT bundles observed by SEM. The DNN molecules should inject the hole carriers in the SWCNTs by the charge transfer interaction and the fundamental charge transport mechanism in the DNN-SWCNT should be the same as the other SWCNTs. The well-known Mott transition of transition metal oxide crystals shows the vertical transition of the electrical conductivity from semiconductor to metal, while the transition is more gradual in the case of disordered solids. [25,26,30] The SWCNT bundles exhibit very sharp diffraction peaks coming from the superlattice structure, as already mentioned above; the superlattice system of the SWCNT bundle is much less crystalline compared with an ordered structure of a single crystalline transition metal oxide and the localized states in the SWCNT bundles should be not uniform. In particular, the superlattice structure of N- or ND molecules-intercalated SWCNT bundles is more disordered, as shown by X-ray diffraction, leading to a widely distributed localized state for electrons. Hence, the Mott transition of N and ND molecules-intercalated SWCNT bundles does not show a vertical change in the temperature dependence of the electrical conductivity.

In the next we need to have an answer for the question why the temperature dependence of the electrical conductivity of ND-adsorbed SWCNT bundles has a maximum, being quite different from the behavior of a well-known metal-semiconductor transition. We must notice that N-adsorbed SWCNT bundles do not have such a maximum in the log σ vs. T^{-1} plot. A great difference of the ND molecule from naphthalene is on the presence of the moieties; the DNN and DHN molecules have two nitro groups and hydroxyl ones. The frame work of the naphthalene molecule has less motional freedom than the functional groups in the SWCNT bundle. The melting points of DNN and DHN are 505 K and 551 K, respectively. Confinement of naphthalene (N), methylnaphthalene (MN), methoxynaphthalene (MeN) and chloronaphthalene (ClN) in the silicious mesopores of SBA-15 of 5.5 nm lowers their melting temperature by 65 K – 85 K. [31] As the confinement of DNN and DHN in the interstices of the SWCNT bundles is much more intensive, the depression of the melting temperature should be more than that in SBA-15. The depression of the melting temperature of DNN inserted in the SWCNT bundles by 200 K predicts an anomaly in the temperature dependence of the electrical conductivity around T = 305 K (T^{-1} = 3.3 x 10^{-3}). Generally speaking, librational and/or rotational motions of moieties of the molecule should start below the melting temperature. The motion of the moieties on the pre-melting process is presumed to expand and fluctuate the intertube distance of the SWCNT bundles, bringing about a depression of the electrical conductivity. If librational or rotational motions of nitro groups of the DNN molecule begin around 250 K, the maximum at 250 K can be understood. We can understand the maximum of log σ vs. T^{-1} plot of DHN-SWCNT in a similar way.

GCMC simulation shows the plausible intercalation configuration and mutual orientational structure of DNN molecules in the pried interstice of the SWCNT bundle estimated by X-ray diffraction data, as shown in Fig.7. DNN molecules align along the interstice between SWCNTS, which should be fit for charge transfer interaction. Thus, the DNN molecules can be intercalated in the SWCNT bundle. The moieties of the DNN molecule should do a librational or rotational motion around the temperature giving the maximum of log σ vs. T^{-1} plot, partially unraveling of the ordered bundle structure and then the electrical conductivity drops above the temperature, as mentioned above. The DHN-adsorbed SWCNT is assumed to have a structure similar to that shown in Fig. 7. Also it is possible that the librational or rotational motion of the moieties of the naphthalene molecules may couple with the theoretically predicted librational motion of SWCNT bundles[10] to induce the observed drop in the electrical conductivity. The newly observed molecular motion-aided electrical conductivity change in this work can be applicable to design a new switching device.

We will compute the electronic structures with the DFT method and get the temperature dependence of the snapshots of ND molecules in the interstitial position of the SWCNT bundle with the GCMC simulation in the future study. Also we need to detect directly the above-mentioned molecular motion with the DSC measurement and observe the ND molecular state with high resolution transmission electron microscopy in future.

4 Conclusions

Naphthalene and its derivatives, 1,5-dinitronaphthalene and 1,5-dihydroxynaphthalene, are partially intercalated in the interstitial positions of the SWCNT bundles, bringing about charge transfer interaction, though the intercalated SWCNT bundles have not necessarily well-ordered structure. The electrical conductivity of these naphthalene and its derivative-intercalated SWCNT bundles except for higher temperature range can be described by the variable range hopping mechanism. The naphthalene and naphthalene derivative-intercalated SWCNT bundles give a metal-semiconductor transition, but the transition is not sharp because of less crystallinity of the superlattice structure of the SWCNT bundles. As1,5-dinitronaphthalene or 1,5-dihydroxynaphthalene as the intercalants has the functional group which can induce a librational motion even in the interstitial position, the conduction path between the SWCNT bundles should be partially broken due to an unraveling of the bundle structure induced by the libration of the intercalant molecules. This mechanism gives an unusual temperature dependence of the electrical conductivity in addition to metal-semiconductor transition characteristics.

Acknowledgements

T. F., M. E., K. K. and M. T. were supported by Exotic Nanocarbons, Japan Regional Innovation Strategy Program by the Excellence, JST. This work was supported by Grant-in-Aid for Scientific Research (A) (24241038) and D. M. was partially supported by JST CREST “Creation of Innovative Functional Materials with Advanced Properties by Hyper-nano-space Design”.

References

1 K. Kaneko, T. Itoh and T. Fujimori, *Chem. Lett.*, 2012, **41**, 466-475.
2 H. E. Romero, K. Bolton, A. Rosen and P.C. Eklund, *Science*, 2005, **307**, 89-93.
3 E. S. Snow , F. K. Perkins, E. J. Houser, S. C. Badescu and T. L. Reinecke, *Science*, 2005, **307**, 1942-1945.
4 A. Star, V. Joshi, S. Skarupo, D. Thomas and J. C. Gabriel, *J. Phys. Chem. B*. 2006, **110**, 21014-21020.
5 Y. Battie, O. Ducloux, P. Thobois, N. Dorval, J. S. Lauret, B. Attal-Tretout and A. Loiseau, *Carbon*, 2011, **49**, 3544-3552.
6 Y. Maniwa, H. Kataura, M. Abe, S. Suzuki, Y. Achiba, H. Kira and K. Matsuda, *J. Phys. Soc. Japan*, 2002, **71**, 2863-2866.
7 F. Khoerunnisa, T. Fujimori, T. Itoh, K. Urita, T. Hayashi, H. Kanoh, T. Ohba, S. Y. Hong, Y. C. Choi, S. J. Santosa, M. Endo and K. Kaneko, *J. Phys. Chem. C*, 2012, **116**, 11216-11222.
8 Y. Hattori, T. Ohba and K. Kaneko, *Comprehensive Inorganic Chemistry II: From Elements to Applications*, Elsevier, 2013, vol. 5. Chap. 5.
9 K. Urita, Y. Shiga, T. Fujimori, Y. Hattori, H, Kanoh, T. Ohba, H. Tanaka, M. Yudasaka, S. Iijima, I. Moriguchi, F. Okino, M. Endo and K. Kaneko, *J. Amer. Chem. Soc*., 2011, **133**, 10344-10347.
10 T. Fujimori, A. Morelos-Gómez, Z. Zhu, H. Muramatsu, R. Futamura, K. Urita, M. Terrones, T. Hayashi, M. Endo, S. Y. Hong, Y. C. Choi, D. Tománek and K. Kaneko, *Nature Comm*., 2013, **4**, 2162-2169
11 D. Noguchi, H. Tanaka, T. Fujimori, T. Kagita, Y. Hattori, H. Honda, K. Urita, S. Utsumi, Z.-M. Wang, T. Ohba, H**.** Kanoh, K. Hata and K. Kaneko, *J. Phys. Condens. Matter.*, 2010, **22,** 334207-334221.
12 H. Marsh, N. Murdie and I. A. S. Edwards, *Chem. Phys. Carbon*, 1987, **20**, 213-272.
13 R. S. Lee, H. J. Kim, J. E. Fischer, A. Thess and R. E. Smalley, *Nature*, 1997, **388**, 255-257.

14 T. Takenobu, T. Takano, M. Shiraishi, Y. Murakami, M. Ata, H. Kataura, Y. Achiba and Y. Iwasa, *Nat. Mater*., 2003, **2**, 683-688.
15 Y.-K. Kwon and D. Tománek, *Phys. Rev. Lett.*, 2000, **84**, 1483-1486.
16 S. Gotovac, H. Honda, Y. Hattori, K. Takahashi, H. Kanoh and K. Kaneko, *Nano Lett*., 2007, **7**, 583-587.
17 M. Arai, S. Utsumi, M. Kanamaru, K. Urita, N. Yoshizawa, D. Noguchi, K. Nishiyama, Y. Hattori, F. Okino, T. Ohaba, H. Tanaka, H. Kanoh and K. Kaneko, *Nano Lett.*, 2009, **9**, 3694-3698.
18 S. Gotovac-Atlagic, T. Hosokai, T. Ohba, N. Ueno, H. Kanoh and K. Kaneko, *Phys. Rev. B,* 2010, **82,** 075136-1～6.
19 F. Khoerunnisa, D. Minami, T. Fujimori, S. Y. Hong, Y. C. Choi, H. Sakamoto, M. Endo and K. Kaneko, *Adsorption*, 2014, **20**, 301-309.
20 H-J. Shin, S. M. Kim, S-M. Yoon, A. Benayad, K. K. Kim, S. J. Kim, H. K. Park, J-Y. Choi and Y. H. Lee, *J. Amer. Chem. Soc*., 2008, **130**, 2062-2066.
21 H. Kataura, Y. Kumazawa, Y. Maniwa, I. Uemzu, S. Suzuki, Y. Ohtsuka and A. Achiba, *Synthetic Metals*, 1999, **103**, 2555-2558.
22 R. B. Weisman and S. M. Bachilo, *Nano Lett.*, 2003, **3**, 1235-1238.
23 A. M. Rao, P. C. Eklund, S. Bandow, A. Thess and R. E. Smalley, *Nature*, 1997, **388**, 257-259.
24 K. Yakushi, M. Oguchi, H. Kuroda, *Bull. Chem. Soc. Jpn*, 1979, **52**, 3180-3191.
25 N. F. Mott and E. A. Davis, *Electronic Processes in Non-Crystalline Materials,* Clarendon Press, Oxford, 1971.
26 N. F. Mott, *Metal-Insulator Transition,* Taylor & Francis, London, 1974.
27 K. Snoussi, A. Vakhshouri, H. Okimoto, T. Takenobu, Y.Iwasa, S. Maruyama, K. Hashimoto and Y. Hirayama, *Phys. Stat. Solid*, 2012, **9**, 183-186.
28 G. T. Kim, E. S. Choi, D. C. Kim, D. S. Suh and Y. W. Park, *Phys. Rev. B*, 1998, **58**, 16064-16 069.
29 S. Luo, T. Liu, S. M. Benjamin and J. S. Brooks, *Langmuir*, 2013, **29**, 8694-8702.
30 P. A. Cox, *Transition Metal Oxides*, Clarendon Press, Oxford, 1995.Chap.5.
31 J. A. Lee, H. Rösner, J. F. Corrigan and Y. Huang, *J. Phys. Chem. C*, 2011, **115**, 4738-4748

Figure Captions

Fig.1 SEM images of SWCNT (A) and DHN-adsorbed SWCNT (B).

Fig.2 X-ray diffraction patterns of SWCNT, N-adsorbed SWCNT and ND-adsorbed SWCNT bundles. Black (a): SWCNT, green (b): N-SWCNT, blue (c): DNN-SWCNT and red (d): DHN-SWCNT

Fig.3 Optical absorption spectra of SWCNT, N-, DNN- and DHN- adsorbed SWCNTs.

Fig. 4 The temperature dependence of electrical conductivity σ of SWCNT samples.

Fig.5 Temperature dependence of electrical conductivity σ around ambient temperature.

Fig. 6 The 3D variable range hopping plots. The electrical conductivity in the lower temperature range gives the best fit for the 3 D plot.

Fig. 7 Plausible intercalated configuration (A) and mutual molecular orientation (B) of DNN molecules in a pried interstice of the SWCNT array. Black; carbon, light grey; hydrogen, red; oxygen and purple; nitrogen

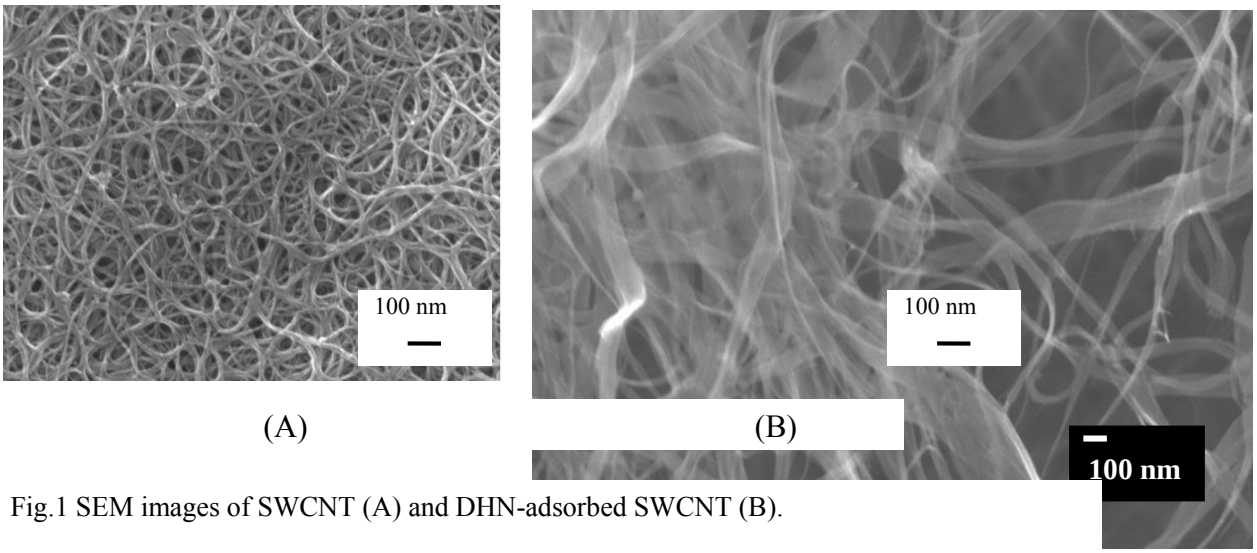

Fig.1 SEM images of SWCNT (A) and DHN-adsorbed SWCNT (B).

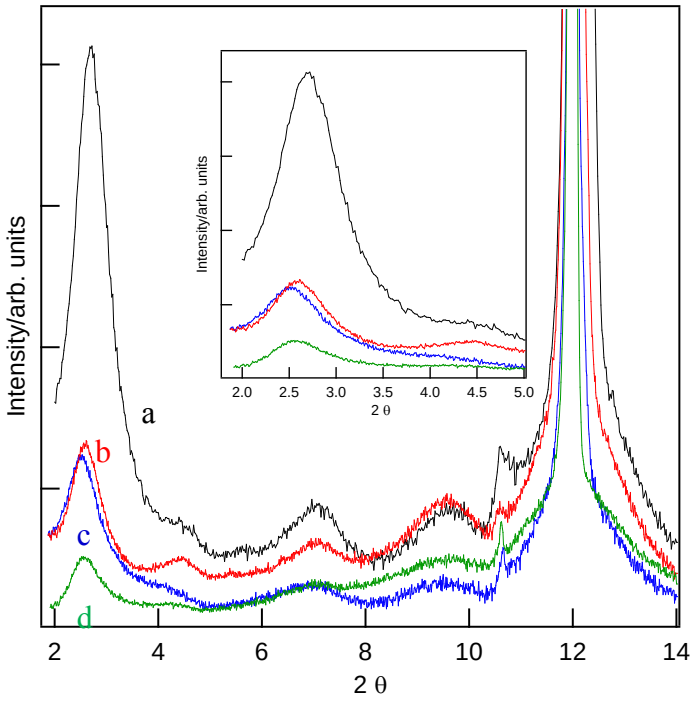

Fig.2 X-ray diffraction patterns of SWCNT, N-adsorbed SWCNT and ND-adsorbed SWCNT bundles. Black (a): SWCNT, green (b): N-SWCNT, blue (c): DNN-SWCNT and red (d): DHN-SWCNT

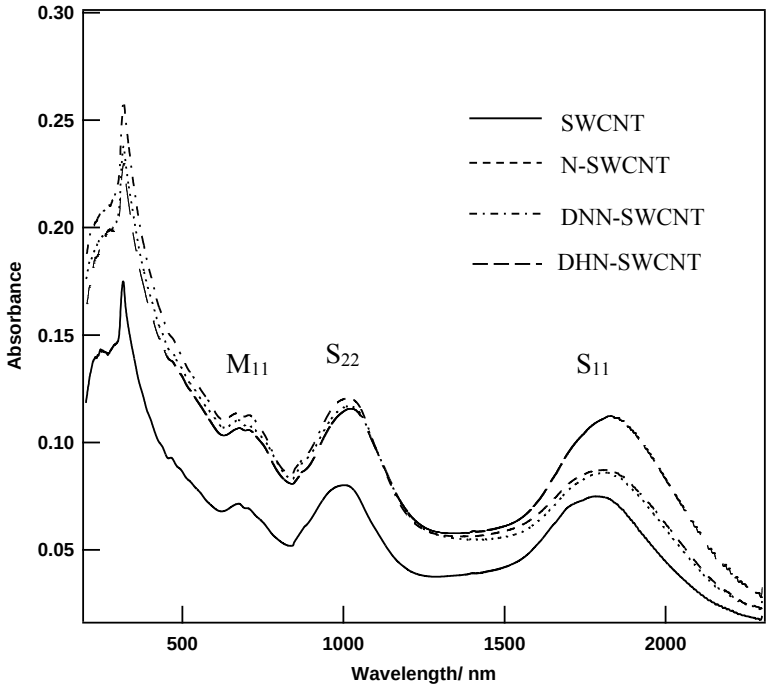

Fig.3 Optical absorption spectra of SWCNT, N-, DNN- and DHN- adsorbed SWCNTs.

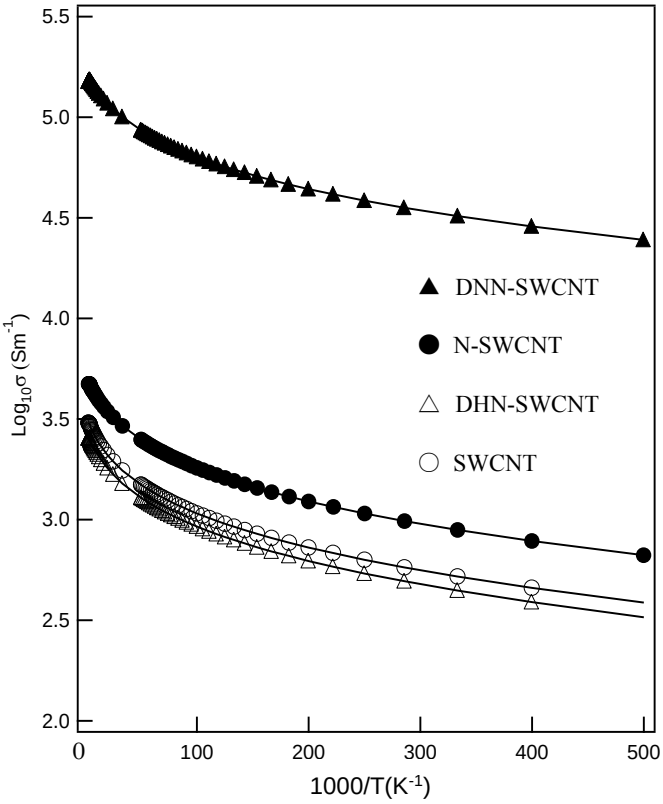

Fig. 4 The temperature dependence of electrical conductivity σ of SWCNT samples.

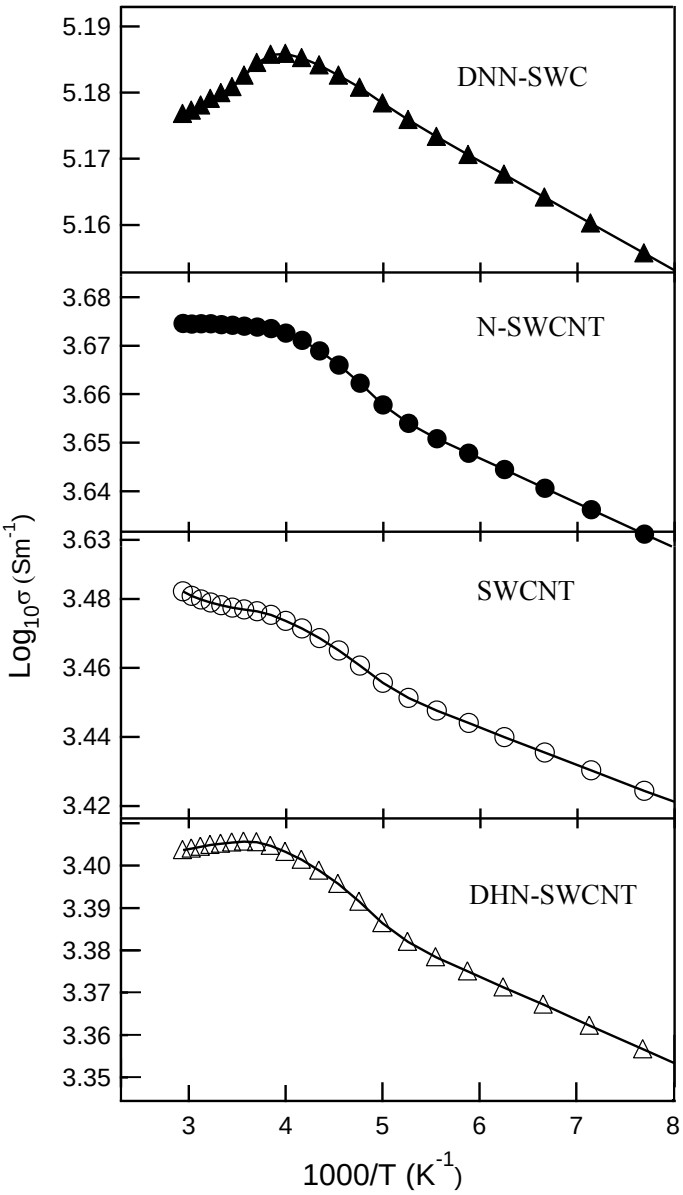

Fig.5 Temperature dependence of electrical conductivity σ around ambient temperature.

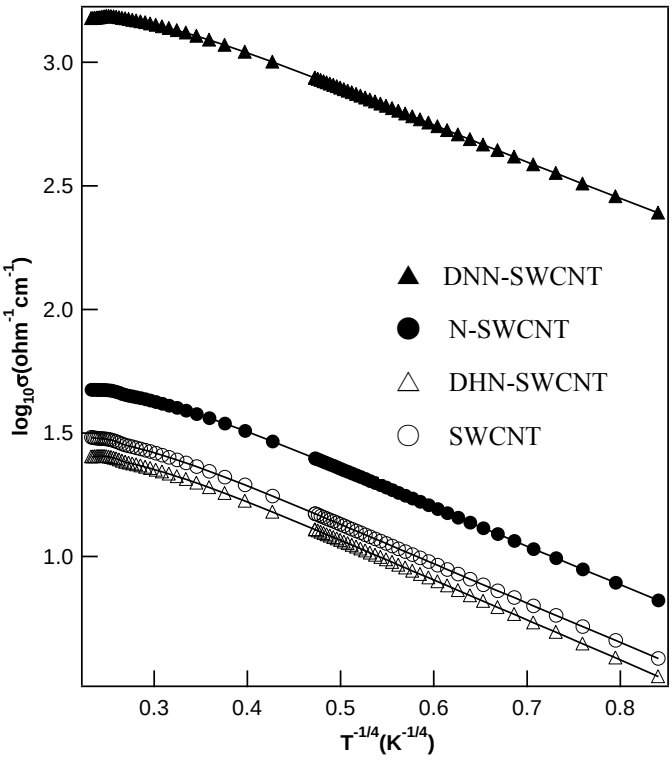

Fig. 6 The 3D variable range hopping plots. The electrical conductivity in the lower temperature range gives the best fit for the 3 D plot.

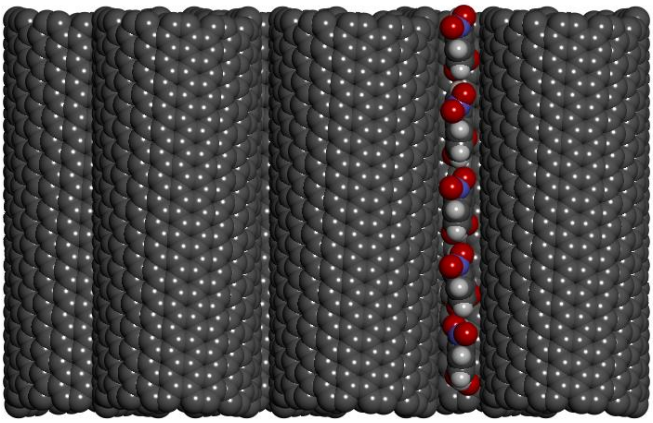

(A)

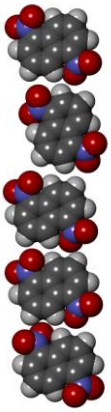

(B)

Fig. 7 Plausible interca
molecules in a pried i
red; oxygen and purple